

**FIB-TEM INVESTIGATION OF AN ALLENDE TYPE A CAI INTERIOR AND THE ASSOCIATED WARK-LOVERING RIM.** Rhonda M. Stroud<sup>1</sup>, Thomas J. Zega<sup>1</sup>, Mariana Cosarinsky<sup>2</sup> and Kevin D. McKeegan<sup>2</sup>, <sup>1</sup>Code 6366 Naval Research Laboratory, Washington DC, 20375 ([stroud@nrl.navy.mil](mailto:stroud@nrl.navy.mil)). <sup>2</sup> Dept. Earth & Space Sciences, UCLA, Los Angeles, CA – 90095-1567.

**Introduction:** The outer boundaries of calcium aluminum rich inclusions (CAIs) typically consist of concentric layers of oxide and silicate minerals, known as Wark-Lovering rims (WLRs). These WLRs are thought to have formed by either flash heating [1] or condensation [2]. In the case of a type A CAI (G4a TS#25) from the Allende CV3 meteorite, isotopic analyses show that WLR formed  $1.3 \times 10^5$  years after the interior, based the well-correlated isochrons in Al-Mg evolution diagrams [3]. In order to further constrain the relationship between the CAI interior and WLR, and the formation conditions of each, we are conducting FIB-enabled, correlated isotope-structure studies. We present herein results of transmission electron microscopy (TEM) studies of interior and WLR sections.

**Methods:** We used an FEI Nova 600 focused ion beam-scanning electron microscope (FIB-SEM) equipped with an Ascend Extreme Access lift-out tool to produce site-specific sections of the CAI and WLR for TEM analysis [4]. The extracted rim section spanning the entire WLR, is approximately 20  $\mu\text{m}$  across by  $\sim 6.5 \mu\text{m}$  deep. The interior section is 21  $\mu\text{m}$  by 7.4  $\mu\text{m}$ . The TEM analysis was carried out with a JEOL 2200FS microscope equipped with a Thermo Noran NSS energy-dispersive spectrometer (EDS), and bright and dark field scanning transmission electron microscopy detectors. The mineral identifications are based on selected area diffraction and EDS results.

**Results and Discussion:** The interior section contained three grains: one each of spinel, hibonite and gehlenite. The grain boundary between the hibonite and spinel is flat, whereas the gehlenite shows round grain boundaries. There is no sign of replacement phases at any of the boundaries. The direction of curvature of these boundaries indicates that the gehlenite was the last to form. Although it is typical for melilite (of which gehlenite is the Al-rich end member) to enclose spinel in type A CAIs, this is inconsistent with the condensation sequence predicted equilibrium thermodynamic calculations [5]. However, it was previously suggested that the kinetics of epitaxial growth of spinel on hibonite can result in spinel condensation temperatures higher than melilite [6], as appears to be the case here.



**Figure 1.** Bright field STEM image of the CAI interior. Sp= spinel, Hib= hibonite, Geh= gehlenite.

Scanning electron microscopy of the WLR shows three layers: an innermost layer of spinel intergrown with hibonite blades and minor perovskite; an intermediate layer of melilite, pervasively replaced by anorthite; and an outermost layer of Ti-Al-rich pyroxene grading outwards to Al-diopside. The TEM analyses of the extracted section (Figure 2) reveal that the layers contain a complex mixture of polycrystalline material. Identified primary phases at increasing distance from the interior include: melilite, anorthite, wollastonite (tentative) and diopside. The grains are primarily sub-hedral in texture with grain sizes of a few microns. However, some grains, e.g., melilite, exhibit triple junctions with surrounding material. Inclusions occur both in and between the melilite and anorthite. Two aqueous alteration products [7], grossular and sodalite, also appear. The sodalite shows abundant radiation tracks. The origin of these tracks could be an important constraint on the timing and location of the aqueous alteration event that produced the sodalite. A solar flare origin would indicate that the hydration most likely occurred in the solar nebula, prior to accretion of the CAI onto the Allende parent body, possibly by mechanism similar to that described by Ciesla et al [8].

#### References:

[1] Wark D. and Boynton W.V. 2001 *Meteoritics and Planetary Science* 36:1135-1166. [2] Simon J.I. et al. 2005 *Earth and Planetary Science Letters* 238:272-283. [3] Cosarinsky M. et al. 2005. *Meteoritics and Planetary Science* 40: A34. [4] Zega T.J. et al. (2007) *Meteoritics and Planetary Science* in press. [5] Ebel D. 2006 in *Meteorites in the Early Solar System II*, 253-277. [6] Beckett J.R. et al. 1994 *Meteoritics* 29:41-65. [7] Krot A. et al. 1995. *Meteoritics and Planetary Science* 30:748-775. [8] Ciesla F.J. et al. 2003 *Science* 200:549-552.

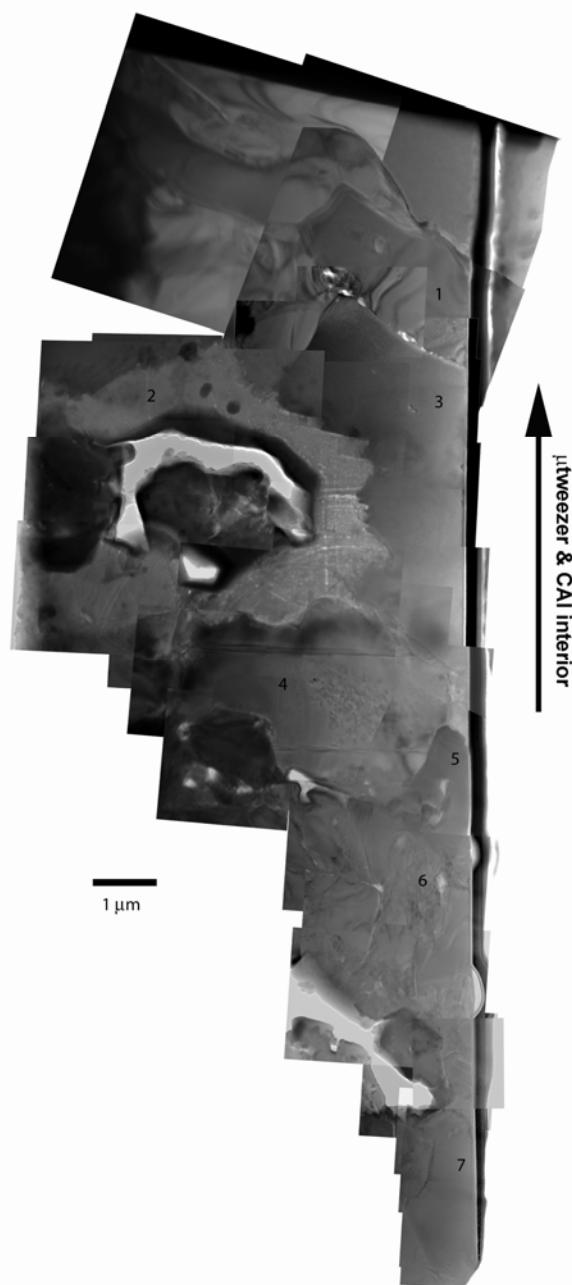


**Figure 2.** TEM mosaic of the Wark-Lovering RIM. The image is a composite of bright field images taken with the individual grains oriented along a crystal zone axis to highlight diffraction contrast features. The phases are: (1) melilite; (2) sodalite; (3) anorthite; (4) anorthite / pyroxene; (5) grossular; (6) wollastonite and (7) diopside. Note the track features (white stripes) in the sodalite.